

EFFICIENT AEROSTRUCTURAL DESIGN OPTIMIZATION COMBINING GRADIENT-ENHANCED KRIGING WITH COUPLED ADJOINT METHOD

Hong-Jiang Guo^{1,2}, Zhong-Hua Han^{1,2,*}, Chen-Zhou Xu^{1,2}, Ke-Shi Zhang^{1,2}, Wen-Ping Song^{1,2}, & Jia-Qi Luo³

¹ Institute of Aerodynamic and Multidisciplinary Design Optimization, School of Aeronautics, Northwestern Polytechnical University, Xi'an, Shaanxi 710072, China

² National Key Laboratory of Aircraft Configuration Design, Xi'an, Shaanxi 710072, China ³ School of Aeronautics and Astronautics, Zhejiang University, Hangzhou, Zhejiang 310027, China

Abstract

Aerostructural design optimization is crucial for green aviation due to its capability of balancing low weight and high aerodynamic performance. However, aerostructural design optimization suffers from numerous expensive coupled analyses, each requiring multiple iterations of computational fluid dynamics (CFD) and finite element method (FEM) simulations, as well as data transfers and mesh deformations. To tackle the challenges, an efficient global aerostructural design optimization method combining the gradient-enhanced Kriging (GEK) model with coupled adjoint method is developed. Firstly, the coupled adjoint equations are derived and solved by linear block Gauss—Seidel method. Secondly, the total derivatives are computed and used to assist direct GEK model for the surrogate-based optimization. Finally, the GEK-based optimization method is verified against analytical test case and applied to aerostructural design optimizations of 36-dimensional Drag Prediction Workshop W1 (DPW-W1) and 72-dimensional NASA Common Research Model (CRM) wings. It is observed that, GEK method using coupled adjoint gradient information is much more efficient than traditional Kriging method only using response information.

Keywords: aerostructural design optimization; coupled adjoint gradient analysis; gradient-enhanced Kriging

1. Introduction

For environmental protection and conservation of resources, the aeronautical research institutions worldwide have proposed higher requirements on flight efficiency and CO₂ emission for future commercial aviation, i.e., the U.S. NASA's 'N+3' program[1] and Europe's 'Clean Sky' program[2]. Specifically, the 'N+3' program sets a target to achieve a 60% reduction in the fuel burn by 2035. To achieve the ambitious goal, it is necessary to improve the flight efficiency and reduce structural mass. Aerostructural design optimization, which is able to strike the best balance of low weight and high aerodynamic performance[4], has been attracting the interest of both research and industry for the last fifty years.

Haftka firstly conducted aerostructural optimization using low-fidelity analytical model and Newton's optimization algorithm[5]. With the development of higher-fidelity modelling in both structures and aerodynamics, coupled computational fluid dynamics (CFD) and finite element method (FEM) have been proposed and adopted in aerostructural design optimization. Maute et al.[6] developed a nonlinear block Gauss—Seidel method with relaxation to solve the coupled Euler CFD and linear FEM model. And a direct method was developed to compute gradients, which is proportional to the number of design variables. Martins et al.[7] developed an adjoint method for the coupled system using Euler CFD and linear FEM. The cost of computing gradients using the coupled adjoint method was nearly independent of the number of design variables, which greatly motivated the development of high-dimensionality aerostructural design optimization. Subsequently,

Kenway et al.[8] accomplished it using Reynolds-averaged Navier–Stokes (RANS) CFD and a detailed FEM model.

There are three kinds of numerical optimization methods for the CFD and FEM-based aerostructural design. The first is gradient-based method. It is efficient especially when the gradients of objective and constraint functions are computed by the coupled adjoint method. It can deal with the optimization problem with 100-1000 design variables or even more. However, gradient-based method is sensitive to the initial guesses and easily trapped into local minimum for the multimodal problem. The second is metaheuristic optimization, such as the genetic algorithms (GAs), particle swarm algorithm, etc. It has capability of global optimization, the required number of aerostructural coupled evaluations increases quadratically with the dimensionality of the design variables, which makes the method unsuitable for the expensive aerostructural design optimization. The third is surrogate-based optimization (SBO) method, which is able to find the global optimum within a very limited number of expensive aerostructural coupled evaluations [9,10,11]. For a global expensive optimization problem, SBO can be much more efficient than existing metaheuristic approaches. And for the local optimization problems with number of design variables less than around 15, SBO can be as efficient as the gradient-based optimization based on the adjoint method [12].

Although SBO has proved very promising, it suffers from the curse of dimensionality [13]. The number of expensive evaluations required to build a sufficiently accurate surrogate model increases exponentially with dimensionality, making the computational costs prohibitive for high-dimensional optimization problems. To ameliorate the curse of dimensionality, a surrogate model enhanced by lower-fidelity or gradients information, is of great interest. Gradient-enhanced Kriging (GEK) [14,15,16] is an effective solution that can fully utilize the gradient information to significantly improve the precision of the surrogate model and reduce the number of expensive evaluations required for optimization. The gradients can be computed efficiently by the coupled adjoint method. Therefore, combining the GEK model with the coupled adjoint method can be highly valuable for the expensive and multimodal aerostructural design optimization.

In this article, an efficient global optimization method for aerostructural design is developed by combining the GEK model with coupled adjoint method. In Section 2, the coupled adjoint equations and GEK model are derived. Section 3 verifies the efficiency of the GEK method against an analytical test case. In Section 4, GEK model with coupled adjoint method is applied to aerostructural design optimizations of 36-dimensional Drag Prediction Workshop W1 (DPW-W1) and 72-dimensional NASA Common Research Model (CRM) wings. Section 5 is for the summary.

2. Methodology

2.1 Coupled Adjoint Gradient Analysis

In the article, the aerodynamic model is solved by ADflow[17,18], a second-order finite-volume CFD solver with a discrete adjoint implementation. And the structural model is solved by Toolkit for Analysis of Composite Structures (TACS)[19], a FEM solver specifically for the shell structures. A nonlinear block Gauss—Seidel method is adopted to solve the coupled system, where the load and displacement data is transferred by using a system of rigid links, as proposed by Brown[20].

The total derivative of the aerostructural objective function I with respect to design variables x can be written as

$$\frac{dI}{dx} = \frac{\partial I}{\partial x} + \left[\frac{\partial I}{\partial w} \quad \frac{\partial I}{\partial u} \right] \left[\frac{\partial w}{\partial x} \right],\tag{1}$$

where the w and u are aerodynamic and structural state variables, respectively. If the solution of the aerostructural analysis is converged, the coupled residual (R_A , R_S) is approximately zero and the total derivative of the residual equations is

$$\begin{bmatrix}
\frac{dR_A}{dx} \\
\frac{dR_S}{dx}
\end{bmatrix} = \begin{bmatrix}
\frac{\partial R_A}{\partial x} \\
\frac{\partial R_S}{\partial x}
\end{bmatrix} + \begin{bmatrix}
\frac{\partial R_A}{\partial w} & \frac{\partial R_A}{\partial u} \\
\frac{\partial R_S}{\partial w} & \frac{\partial R_S}{\partial u}
\end{bmatrix} \begin{bmatrix}
\frac{\partial w}{\partial x} \\
\frac{\partial u}{\partial x}
\end{bmatrix} = 0.$$
(2)

To eliminate the complex $\left[\frac{\partial w}{\partial x} \quad \frac{\partial u}{\partial x} \right]^T$, the total derivative of the objective become

$$\frac{dI}{dx} = \frac{\partial I}{\partial x} - \left[\frac{\partial I}{\partial w} \quad \frac{\partial I}{\partial u} \right] \begin{bmatrix} \frac{\partial R_A}{\partial w} & \frac{\partial R_A}{\partial u} \\ \frac{\partial R_S}{\partial w} & \frac{\partial R_S}{\partial u} \end{bmatrix}^{-1} \begin{bmatrix} \frac{\partial R_A}{\partial x} \\ \frac{\partial R_S}{\partial x} & \frac{\partial R_S}{\partial x} \end{bmatrix}.$$
(3)

To avoid the matrix inversion operation, a coupled adjoint vector, $\Phi = \begin{bmatrix} \psi^T & \phi^T \end{bmatrix}^T$, is introduced and obtained by solving eq.(4), called coupled adjoint equations

$$\begin{bmatrix} \frac{\partial R_A}{\partial w} & \frac{\partial R_A}{\partial u} \\ \frac{\partial R_S}{\partial w} & \frac{\partial R_S}{\partial u} \end{bmatrix}^T \begin{bmatrix} \psi \\ \varphi \end{bmatrix} = \begin{bmatrix} \frac{\partial I}{\partial w} & \frac{\partial I}{\partial u} \end{bmatrix}^T. \tag{4}$$

To solve the coupled adjoint equations, a linear block Gauss–Seidel method is adopted, which expresses the interdisciplinary coupling as additional forcing terms to the right hand side of each respective adjoint solver, as shown the following equations

$$\left(\frac{\partial \mathbf{R}_{A}}{\partial \mathbf{w}}\right)^{T} \boldsymbol{\psi}^{(k)} = \left(\frac{\partial I}{\partial \mathbf{w}}\right)^{T} - \left(\frac{\partial \mathbf{R}_{S}}{\partial \mathbf{w}}\right)^{T} \boldsymbol{\varphi}^{(k-1)}
\left(\frac{\partial \mathbf{R}_{S}}{\partial \mathbf{u}}\right)^{T} \boldsymbol{\varphi}^{(k)} = \left(\frac{\partial I}{\partial \mathbf{u}}\right)^{T} - \left(\frac{\partial \mathbf{R}_{A}}{\partial \mathbf{u}}\right)^{T} \boldsymbol{\psi}^{(k)} .$$
(5)

With substituting structural residual equation $R_s = Ku - F_s = 0$ into eq. (5) and applying a relaxation factor, the Gauss–Seidel scheme can be expressed as

$$\left(\frac{\partial \mathbf{R}_{A}}{\partial \mathbf{w}}\right)^{T} \triangle \boldsymbol{\psi}^{(k)} = \left(\frac{\partial I}{\partial \mathbf{w}}\right)^{T} + \left(\frac{\partial \mathbf{F}_{S}}{\partial \mathbf{w}}\right)^{T} \boldsymbol{\varphi}^{(k-1)} - \left(\frac{\partial \mathbf{R}_{A}}{\partial \mathbf{w}}\right)^{T} \boldsymbol{\psi}^{(k-1)}, \qquad \boldsymbol{\psi}^{(k)} = \boldsymbol{\psi}^{(k-1)} + \omega \triangle \boldsymbol{\psi}^{(k)}$$

$$K \triangle \boldsymbol{\varphi}^{(k)} = \left(\frac{\partial I}{\partial \boldsymbol{u}}\right)^{T} - \left(\frac{\partial \mathbf{R}_{A}}{\partial \boldsymbol{u}}\right)^{T} \boldsymbol{\psi}^{(k)} - \left(\frac{\partial \mathbf{F}_{S}}{\partial \boldsymbol{u}}\right)^{T} \boldsymbol{\varphi}^{(k-1)} - \left(K\boldsymbol{\varphi}^{(k-1)}\right), \qquad \boldsymbol{\varphi}^{(k)} = \boldsymbol{\varphi}^{(k-1)} + \omega \triangle \boldsymbol{\varphi}^{(k)} \quad . \tag{6}$$

Once we have solved the eq. (6) for each function, total derivative with respect to all the design variables can be computed by eq. (7). Therefore, the cost of computing gradient by the adjoint method is independent to the number of design variables but proportional to the number of objective functions. On the contrast, if we directly solve eq. (2) for each design variables to obtain the $\left[\partial w/\partial x \ \partial u/\partial x\right]^T$, the total derivative can also be computed by substituting $\left[\partial w/\partial x \ \partial u/\partial x\right]^T$ into eq. (1). However, the cost is proportional to the number of design variables and is independent to the number of design variables. This is known as the direct method. In this article, since the number of design variables is much more than the objective functions, the adjoint method is adopted.

$$\frac{dI}{d\mathbf{x}} = \frac{\partial I}{\partial \mathbf{x}} - \begin{bmatrix} \boldsymbol{\psi} \\ \boldsymbol{\varphi} \end{bmatrix}^T \begin{bmatrix} \frac{\partial \mathbf{R}_A}{\partial \mathbf{x}} \\ \frac{\partial \mathbf{R}_S}{\partial \mathbf{x}} \end{bmatrix} = \frac{\partial I}{\partial \mathbf{x}} - \boldsymbol{\psi}^T \frac{\partial \mathbf{R}_A}{\partial \mathbf{x}} - \boldsymbol{\varphi}^T \frac{\partial \mathbf{R}_S}{\partial \mathbf{x}} \tag{7}$$

2.2 Gradient-Enhanced Kriging

For a m-dimensional problem, the sampled data sets (S, y_s) for modeling GEK are collected as

$$\mathbf{S} = \begin{bmatrix} \mathbf{x}^{(1)} \cdots \mathbf{x}^{(n)} & \mathbf{x}^{(1)} \cdots \mathbf{x}^{(1)} \cdots \mathbf{x}^{(n)} \cdots \mathbf{x}^{(n)} \end{bmatrix}^{T} \in \mathbb{R}^{(n+nm) \times m}$$

$$\mathbf{y}_{\mathbf{S}} = \begin{bmatrix} y^{(1)} \cdots y^{(n)} & \frac{\partial y^{(1)}}{\partial x_{1}} \cdots \frac{\partial y^{(1)}}{\partial x_{m}} \cdots \frac{\partial y^{(n)}}{\partial x_{1}} \cdots \frac{\partial y^{(n)}}{\partial x_{m}} \end{bmatrix}^{T} \in \mathbb{R}^{n+nm} ,$$
(8)

where the gradients in y_s are computed by the coupled adjoint method.

Assume a random process corresponding to GEK

$$\begin{cases} Y(\mathbf{x}) = \beta_0 + Z(\mathbf{x}) \\ \frac{\partial Y(\mathbf{x})}{\partial \mathbf{x}_k} = \frac{\partial Z(\mathbf{x})}{\partial \mathbf{x}_k}, k = 1, \dots, m \end{cases}$$
(9)

where β_0 is a constant and Z(x) is a stationary random process having zero mean and covariance of

$$\begin{cases}
Cov \left[Z\left(\mathbf{x}^{(i)}\right), Z\left(\mathbf{x}^{(j)}\right) \right] = \sigma^{2}R\left(\mathbf{x}^{(i)}, \mathbf{x}^{(j)}\right) \\
Cov \left[Z\left(\mathbf{x}^{(i)}\right), \frac{\partial Z\left(\mathbf{x}^{(j)}\right)}{\partial x_{k}^{(j)}} \right] = \sigma^{2} \frac{\partial R\left(\mathbf{x}^{(i)}, \mathbf{x}^{(j)}\right)}{\partial x_{k}^{(j)}} \\
Cov \left[\frac{\partial Z\left(\mathbf{x}^{(i)}\right)}{\partial x_{l}^{(i)}}, Z\left(\mathbf{x}^{(j)}\right) \right] = \sigma^{2} \frac{\partial R\left(\mathbf{x}^{(i)}, \mathbf{x}^{(j)}\right)}{\partial x_{l}^{(i)}} \\
Cov \left[\frac{\partial Z\left(\mathbf{x}^{(i)}\right)}{\partial x_{l}^{(i)}}, \frac{\partial Z\left(\mathbf{x}^{(j)}\right)}{\partial x_{k}^{(j)}} \right] = \sigma^{2} \frac{\partial^{2}R\left(\mathbf{x}^{(i)}, \mathbf{x}^{(j)}\right)}{\partial x_{l}^{(i)}\partial x_{k}^{(j)}} .
\end{cases} (10)$$

GEK model is an interpolation model using response and gradient values at samples and is expressed as

$$\hat{y}(\mathbf{x}) = \sum_{i=1}^{n} w^{(i)} y^{(i)} + \sum_{j=1}^{m} \sum_{i=1}^{n} \lambda_{j}^{(i)} \frac{\partial y^{(i)}}{\partial x_{j}} = \widetilde{\mathbf{w}}^{T} \mathbf{y}_{s} , \qquad (11)$$

where $\widetilde{\mathbf{w}} = \left[w^{(1)} \cdots w^{(n)} \ \lambda_1^{(1)} \cdots \lambda_m^{(1)} \cdots \lambda_n^{(n)} \cdots \lambda_m^{(n)} \right]^T \in \mathbb{R}^{n+nm}$ is the weight coefficients and obtained by solving the following optimization problem

min.
$$MSE[\hat{y}(x)] = E[(\widetilde{\mathbf{w}}^T \mathbf{Y}_S - Y(x))^2]$$

s.t. $\overline{\mathbf{F}}^T \widetilde{\mathbf{w}} = 1$. (12)

After determining the weight coefficients, the resulting GEK predictor and the mean square error (MSE) is of the form

$$\hat{y}(x) = \widetilde{\mathbf{w}}^{T} \mathbf{y}_{S} = \beta_{0} + \overline{\mathbf{r}}^{T}(x) \underbrace{\overline{\mathbf{R}}^{-1}(\mathbf{y}_{S} - \beta_{0}\overline{\mathbf{F}})}_{V_{GEK}}$$

$$MSE \{\hat{y}(x)\} = \sigma^{2} \left[1 - \overline{\mathbf{r}}^{T} \overline{\mathbf{R}}^{-1} \overline{\mathbf{r}} + \frac{(1 - \overline{\mathbf{F}}^{T} \overline{\mathbf{R}}^{-1} \overline{\mathbf{r}})^{2}}{\overline{\mathbf{F}}^{T} \overline{\mathbf{R}}^{-1} \overline{\mathbf{F}}} \right]$$

$$\overline{\mathbf{R}} = \begin{bmatrix} \mathbf{R} & \partial \mathbf{R} \\ \partial \mathbf{R}^{T} & \partial^{2} \mathbf{R} \end{bmatrix} \in \mathbb{R}^{(n+nm)\times(n+nm)}$$

$$\overline{\mathbf{F}} = \underbrace{\begin{bmatrix} 1 \cdots 1 & 0 \cdots 0 \\ nm \end{bmatrix}}_{nm}^{T} \in \mathbb{R}^{n+nm}$$

$$\overline{\mathbf{r}} = \begin{bmatrix} \mathbf{r} \\ \partial \mathbf{r} \end{bmatrix} \in \mathbb{R}^{n+nm} ,$$
(13)

where Gaussian function and cubic spline function are often employed as the correlation function $R\left(\mathbf{x}^{(i)},\mathbf{x}^{(j)}\right) = \prod_{k=1}^{m} R_k\left(\theta_k,x_k^{(i)}-x_k^{(j)}\right)$, as shown in eq. (14) and (15), respectively.

$$R_{k}\left(\theta_{k}, x_{k}^{(i)} - x_{k}^{(j)}\right) = exp\left(-\theta_{k}\left(x_{k}^{(i)} - x_{k}^{(j)}\right)^{2}\right)$$
(14)

$$R_{k}\left(\theta_{k}, x_{k}^{(i)} - x_{k}^{(j)}\right) = \begin{cases} 1 - 15\xi_{k}^{2} + 30\xi_{k}^{3}, & 0 \le \xi_{k} \le 0.2\\ 1.25\left(1 - \xi_{k}\right)^{3}, & 0.2 < \xi_{k} \le 1\\ 0, & \xi_{k} > 1 \end{cases}$$

$$\xi_{k} = \theta_{k} \left| x_{k}^{(i)} - x_{k}^{(j)} \right|, k = 1, 2, \dots, m$$

$$(15)$$

The model parameters $eta_0, \sigma^2, heta$ are obtained by maximizing logarithm likelihood function

$$\ln(\tilde{L}) = -\frac{n+nm}{2}\ln(2\pi\sigma^2) - \frac{1}{2}\ln|\overline{\mathbf{R}}| - \frac{1}{2}\frac{(\mathbf{y}_s - \beta_0\overline{\mathbf{F}})^T\overline{\mathbf{R}}^{-1}(\mathbf{y}_s - \beta_0\overline{\mathbf{F}})}{\sigma^2}.$$
 (16)

We can get the analytical optima

$$\begin{cases}
\beta_0 = \left(\overline{\mathbf{F}}^T \overline{\mathbf{R}}^{-1} \overline{\mathbf{F}}\right)^{-1} \overline{\mathbf{F}}^T \overline{\mathbf{R}}^{-1} \mathbf{y}_{\mathbf{s}} \\
\sigma^2 = \frac{1}{n + nm} \left(\mathbf{y}_{\mathbf{s}} - \beta_0 \overline{\mathbf{F}}\right)^T \overline{\mathbf{R}}^{-1} \left(\mathbf{y}_{\mathbf{s}} - \beta_0 \overline{\mathbf{F}}\right)
\end{cases}$$
(17)

For the optimal θ , we have to use numerical optimization algorithm to maximize the concentrated joint logarithm likelihood function

$$\theta = \arg \max \left[-(n + nm) \ln \left(\sigma^2 \right) - \ln \left| \overline{\mathbf{R}} \right| \right]. \tag{18}$$

3. Analytical Function Test Case

The 20, 50, and 100-dimensional Rosenbrock functions are used to verify the efficiency of GEK method compared to traditional Kriging method. The optimization model is formulated as:

min.
$$f(\mathbf{x}) = \sum_{i=1}^{m-1} \left[100 \left(x_{i+1} - x_i^2 \right)^2 + \left(1 - x_i \right)^2 \right]$$

w.r.t. $x_i \in [0, 2], \forall i \in [1, m] (m = 20, 50, 100)$. (19)

Each experiment is repeated 10 times with different training samples. The comparison of the

EFFICIENT AEROSTRUCTURAL DESIGN OPTIMIZATION METHOD COMBINING GEK MODEL WITH COUPLED ADJOINT METHOD

convergence curve is shown in Fig. 1. Table 1 shows that the GEK method always obtains lower objective value with fewer number of evaluations. With the increasing of dimensionality, the GEK method does not require more computational cost to achieve the optimal solution which means the GEK method is promising in high-dimensional optimization problems.

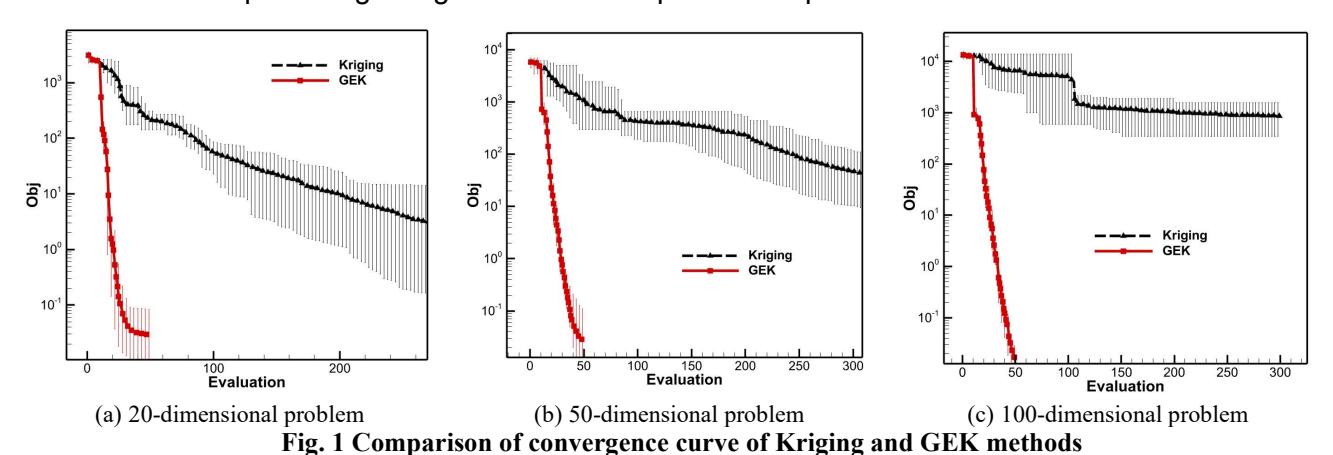


Table 1 Comparison of the optimized results of Kriging and GEK methods (F and G represent the number of function and gradient evaluations respectively)

Number of dimensions Average optimal value Computational cost Theoretical optimal value 1.4267 500F Kriging method 20 **GEK** method 0.0294 50F + 50GKriging method 9.5460 500F 50 **GEK** method 0.026950F + 50GKriging method 869.2719 300F 100 **GEK** method 0.0170 50F + 50G

4. Application to Aerostructural Design Optimization

4.1 Validation of numerical methods and codes

The High Reynolds Number Aero-Structural Dynamics (HIRENASD) benchmark is used to verify the precise of aeroelastic analysis codes developed in this article. The flow condition is $Re = 7.0 \times 10^6$, Ma = 0.7, and the attack of angle is 1.5° . The aerodynamic and structural grids are shown in Fig. 2. The aeroelastic analysis results obtained by the code agree well with the test data, as shown in Fig. 3.

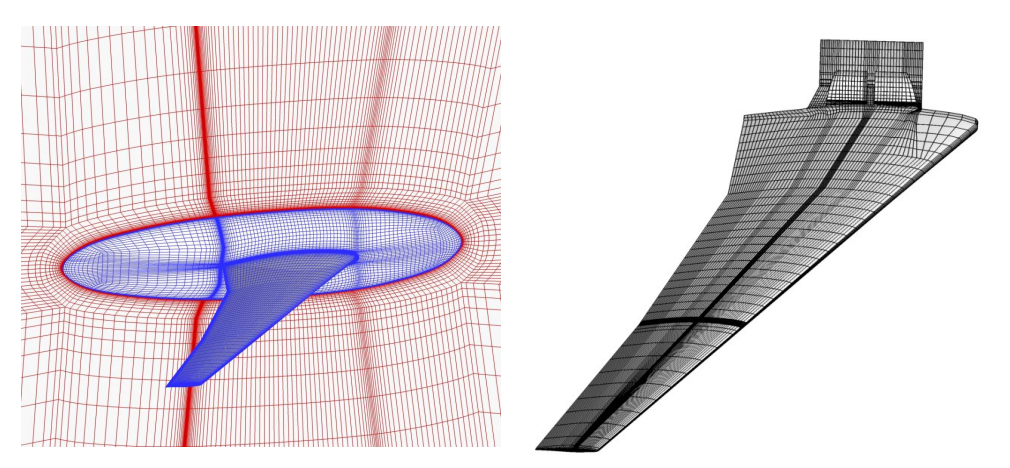


Fig. 2 Aerodynamic (3,088,384 cells) and structural (41,923 elements) grids of HIRENASD

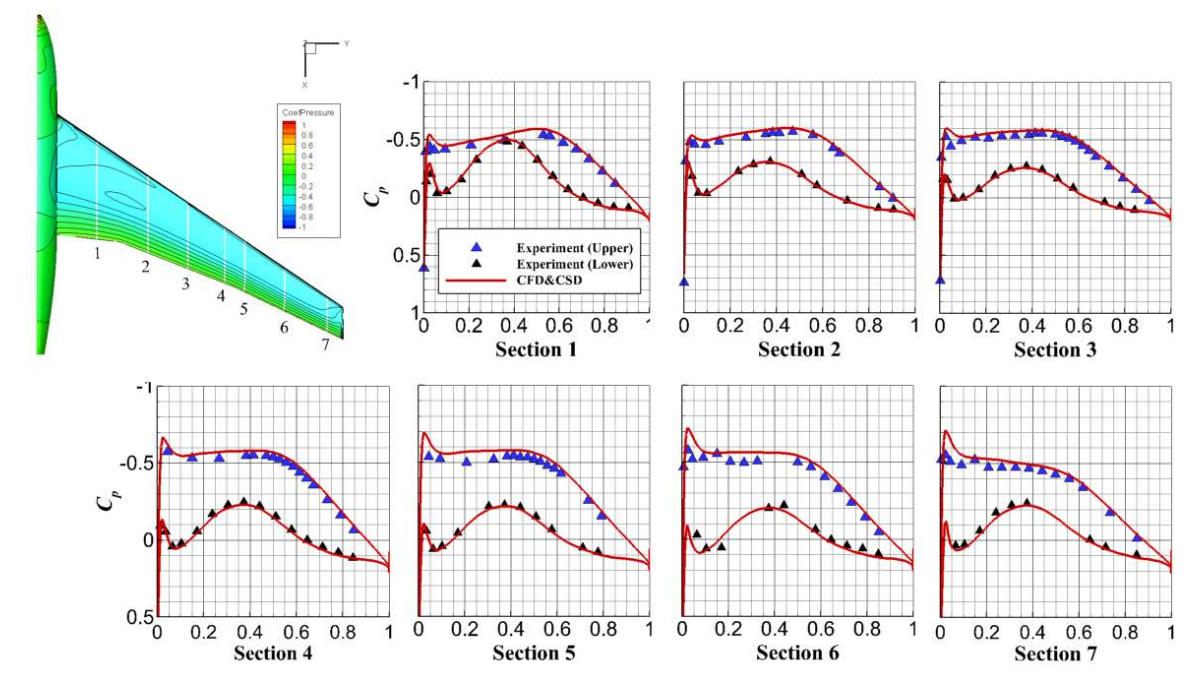


Fig. 3 The comparison of pressure distribution of aeroelastic analysis results and test data

The Drag Prediction Workshop W1 (DPW-W1) wing is used to verify the precision of coupled adjoint gradient analysis code. The flow condition is $Re = 5.0 \times 10^6$, Ma = 0.76, and the attack of angle is 0.5° . The structural model is composed of an upper and lower skin, two spars, 17 ribs and 12 leading- and trailing-edge lumped masses which are used to model the effect of the mounted actuators and control surfaces, as shown in Fig. 4. The aerodynamic and structural models are integrally parameterized by FFD control volume, as shown in Fig. 5. The gradient of force coefficient, mass functions, and Kreisselmeier–Steinhauser (KS) function of element stresses with respect to aerodynamic shape and structural thickness variables are computed by the coupled adjoint and finite-difference methods. Results show that the developed coupled adjoint code has a high precision, and the relative error is less than 5%, as shown in Fig. 6.

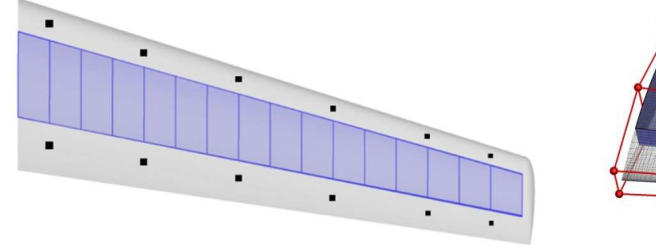
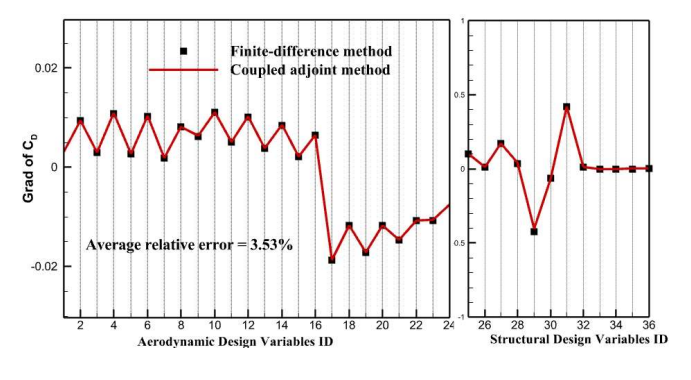


Fig. 4 Aerostructural analysis model of DPW-W1 wing



(a) The gradient of drag coefficient function

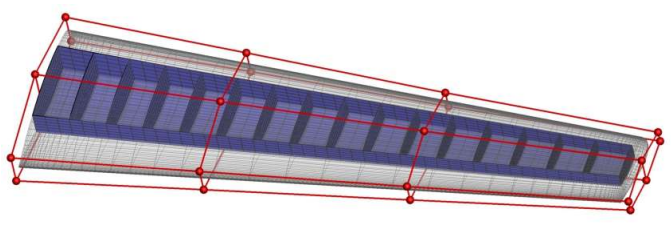
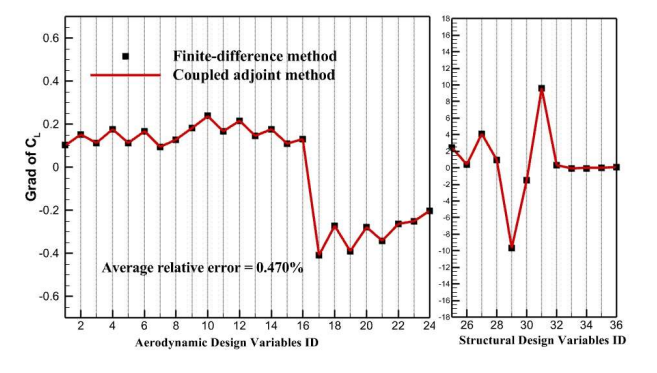
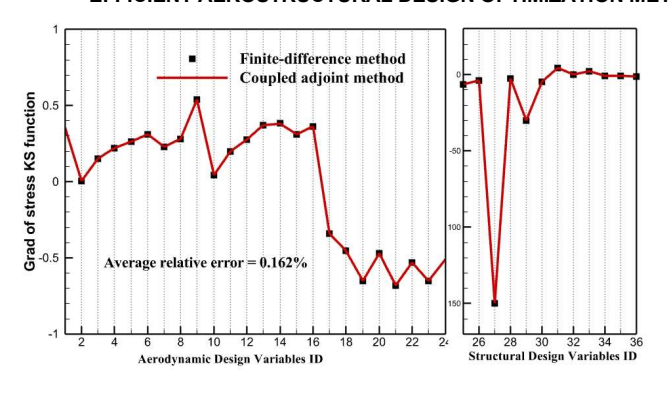
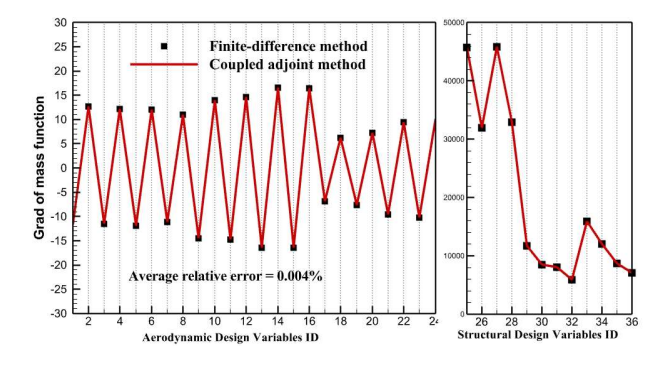


Fig. 5 The aerostructural model is integrally parameterized by FFD control volume



(b) The gradient of lift coefficient function





- (c) The gradient of KS function of element stresses
- (d) The gradient of structural mass function

Fig. 6 Comparison of the gradients computed by finite-difference (FD) and coupled adjoint (AD) methods (where the relative error = $\frac{AD - FD}{FD} \times 100\%$)

4.2 Aerostructural design optimization of DPW-W1 wing

The geometric model of DPW-W1 wing is provided by 3rd AIAA CFD drag prediction workshop. The optimization model is defined as Table 2. To balance the low weight and high aerodynamic performance, the objective is defined as a weighted sum of weight reduction and drag reduction. The constraints include a lift, a trim, and three yield failure constrains. The yield failure margin of each element is computed by using von Mises failure criterion. And the three failure constrains are computed by approximating the maximum failure margin within spar, skin and rib respectively using a Kreisselmeier-Steinhauser (KS) aggregation. The design variables include aerodynamic shape parameterized by 24 FFD control points and 12 structural thickness of ribs, spars and skins, as shown in Fig. 7.

Table 2 Aerostructural optimization model of DPW-W1 wing

Optimization objective/constrains/ variables	Description	Quantity
Min. $\omega \cdot \frac{C_D - C_{D0}}{\Delta C_D} + (1 - \omega) \cdot \frac{W - W_0}{\Delta W}$	weighted sum of weight reduction and drag reduction	1
$s.t. C_L / C_{L0} \ge 1.0$	Lift coefficient constrain	1
$\left C_{M} / C_{M0} \right \leq 1.0$	Moment coefficient constrain	1
$KS_{ribs} \le 1.0$	Rib yield failure constrain	1
$KS_{skins} \le 1.0$	Skin yield failure constrain	1
$KS_{spars} \le 1.0$	Spar yield failure constrain	1
$t/t_{initial} \ge 1.0$	Geometric thickness constrains	8
w.r.t. x _{shape}	FFD control points	24
$oldsymbol{x}_{thickness}$	Structural panel thickness	12

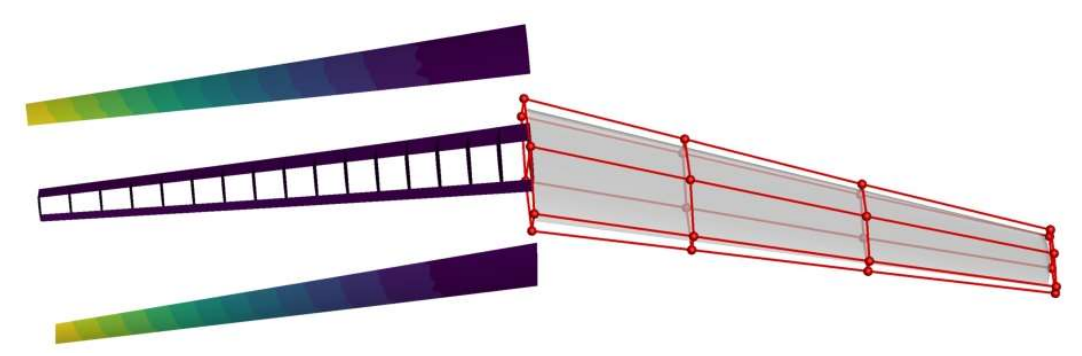


Fig. 7 The aerostructural optimization includes 12 structural thickness and 24 aerodynamic shape design variables

Two optimization methods are investigated and adopted to perform the optimization. 1) Kriging method only using response information; 2) GEK method using coupled adjoint gradient information. Among them, expected improvement (EI) infilling-sampling criteria, known as efficient

EFFICIENT AEROSTRUCTURAL DESIGN OPTIMIZATION METHOD COMBINING GEK MODEL WITH COUPLED ADJOINT METHOD

global optimization (EGO), is adopted and the models are repeatedly update with response and coupled adjoint gradient data of the new samples during the optimization.

The results are shown in Fig. 8 and Table 3. The comparison shows that the result of GEK method is much better than that of Kriging method. Meanwhile, GEK method require much fewer iterations and aerostructural coupled analyses compared to Kriging method.

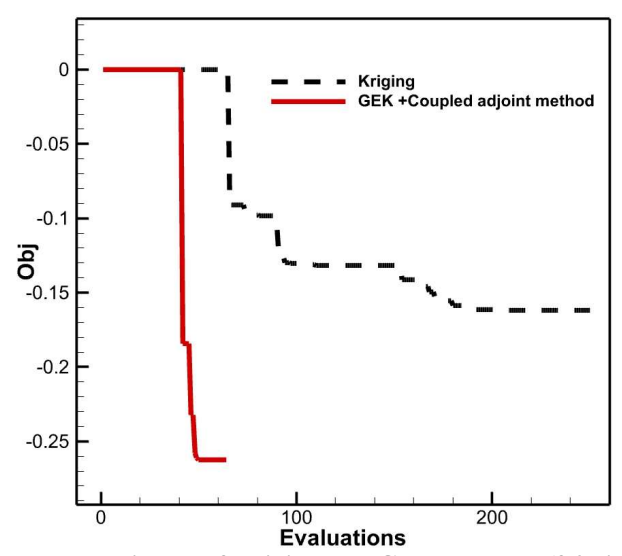


Fig. 8 Convergence history of Kriging and GEK methods (36-dimensional)

Table 3 Results and computational cost of Kriging and GEK methods (36-dimensional, F and G represent the number of function and gradient evaluations respectively)

	Objective function	Computational cost
Kriging method	-0.1690	250F
GEK + Coupled adjoint method	-0.2623	64F+64G

Fig. 9 shows the comparison of the pressure distribution and sectional airfoils between baseline and optimized wings. Table 4 shows the analysis results of baseline and optimized wings. It is observed that drag coefficient and structural mass of the wing optimized by GEK method are reduced by 4 counts (-2.3%) and 310 kg (-18.7%).

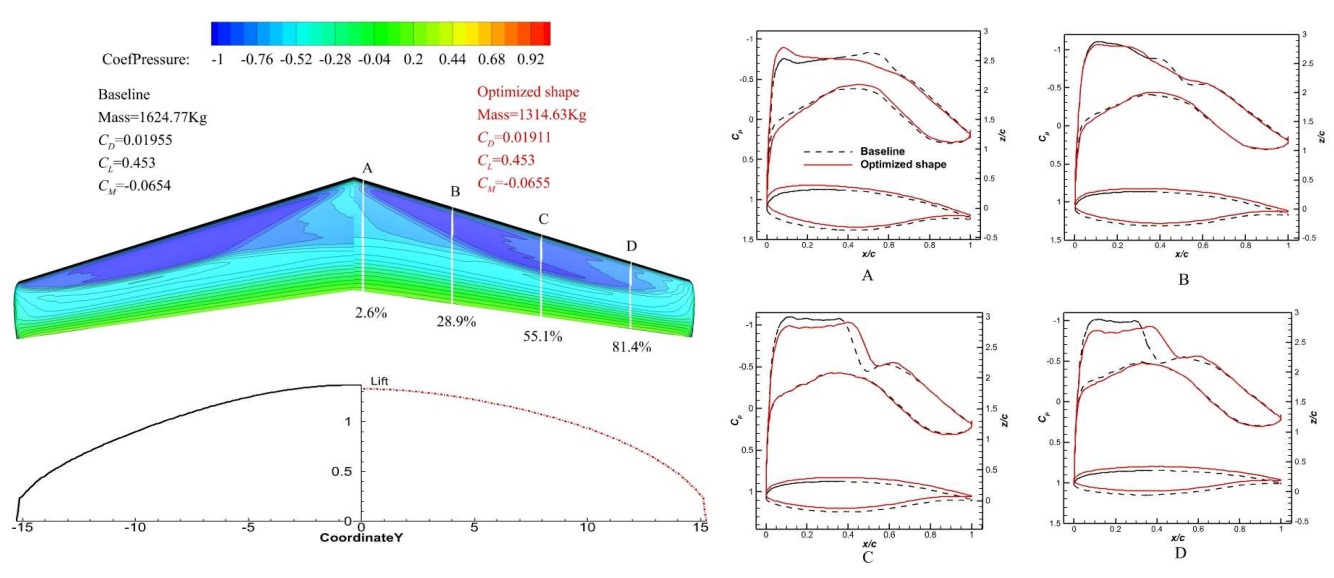


Fig. 9 The comparison of pressure distribution and sectional airfoils between baseline and optimized wings ($Re = 5.0 \times 10^6$, Ma = 0.76, $AoA = 0.5^\circ$)

Table 4 The aerostructural analysis results of baseline and optimized wings

Quantity	Baseline	Kriging optimization	GEK optimization
Drag coefficient C_D	0.01955	0.01920 (-1.8%)	0.01911 (-2.3%)
Total wing Mass, Kg	1624.77	1611.88 (-0.8%)	1320.25 (-18.7%)
Lift coefficient C_L	0.453	0.453	0.453
Moment coefficient C_M	-0.0654	-0.0654	-0.0655
Stress K-S ribs	0.079	0.149	0.115
Stress K-S skins	0.470	0.572	0.589
Stress K-S spars	0.406	0.511	0.698

4.3 Aerostructural design optimization of CRM wing

The NASA CRM has been used in the AIAA DPWs for validating CFD methods since 2009. In this article, the CRM wing is used to verify the developed aerostructural design optimization method. The flow condition is $Re = 5.0 \times 10^6$, Ma = 0.85, $C_L = 0.5$. The aerostructural analysis model is shown in Fig. 10. The optimization model is shown in Table 5. The number of design variables is increased to 72 with 56 aerodynamic shape and 16 structural thickness variables. The objective is similar to the DPW-W1 case, and the constrains are simplified.

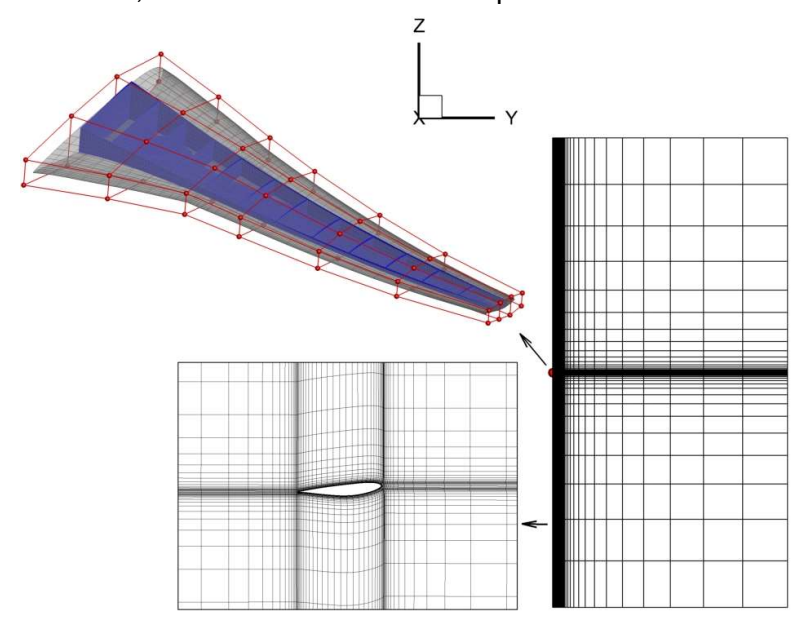


Fig. 10 Aerostructural analysis model of CRM wing

Table 5 Aerostructural optimization model of CRM wing

Table 5 Aerostructural optimization model of CKM wing			
Optimization objective/constrains/ variables	Description	Quantity	
Min. $\omega \cdot \frac{C_D - C_{D0}}{\Delta C_D} + (1 - \omega) \cdot \frac{W - W_0}{\Delta W}$	weighted sum of weight reduction and drag reduction	1	
$s.t. C_L / C_{L0} \ge 1.0$	Lift coefficient constrain	1	
$\left C_{M} / C_{M0} \right \leq 1.0$	Moment coefficient constrain	1	
$KS_{stress} \le 1.0$	Structural yield failure constrain	1	
w.r.t. \mathbf{x}_{shape}	FFD control points	56	
$oldsymbol{\mathcal{X}}_{thickness}$	Structural panel thickness	16	

EFFICIENT AEROSTRUCTURAL DESIGN OPTIMIZATION METHOD COMBINING GEK MODEL WITH COUPLED ADJOINT METHOD

The optimization is also conducted by Kriging and GEK methods. The results are shown in Fig. 11 and Table 6. GEK method using coupled adjoint gradient information converges quickly and obtains a lower objective function value with fewer computational cost.

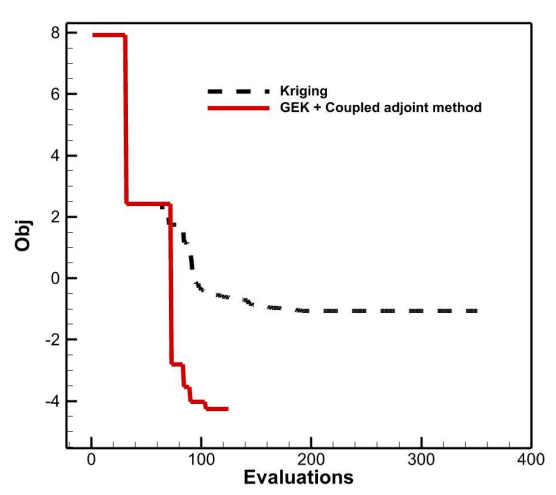


Fig. 11 Convergence history of Kriging and GEK methods (72-dimensional)

Table 6 Results and computational cost of Kriging and GEK methods (72-dimensional, F and G represent the number of function and gradient evaluations respectively)

	Objective function	Computational cost
Kriging method	-1.0695	351F
GEK + coupled adjoint method	-4.2630	104F+104G

Fig. 12 shows the comparison of the pressure distribution and sectional airfoils between baseline and optimized wing by GEK method. Table 7 shows that drag coefficient and structural mass of the wing optimized by GEK method are reduced by 53 counts (-18.3%) and 79 kg (-3.3%), which is much better than that of the wing optimized by traditional Kriging method whose aerodynamic performance is improved limitedly and structural mass is even increased.

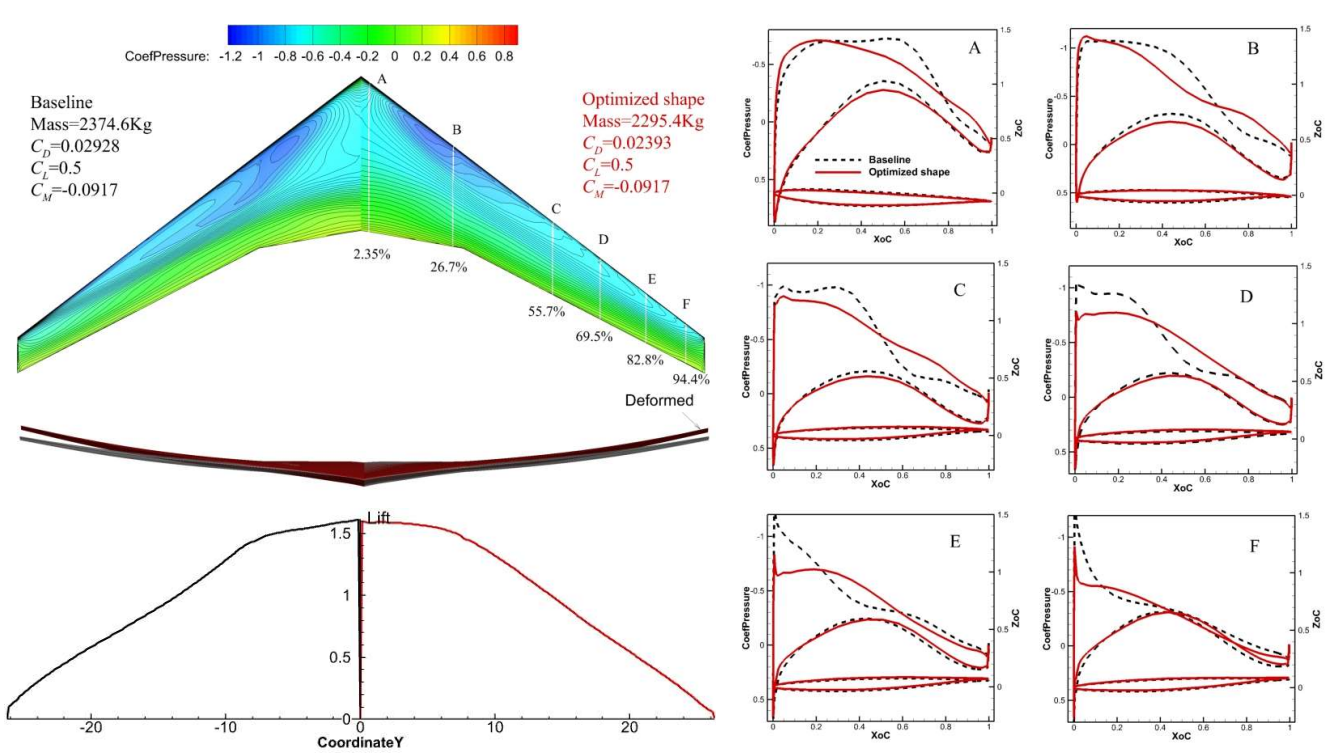


Fig. 12 The comparison of pressure distribution and sectional airfoils between baseline and optimized wing by GEK method ($Re = 5.0 \times 10^6$, Ma = 0.85, $C_L = 0.5$)

Table 7 The aerostructural analysis results of baseline and optimized wings ($Re = 5.0 \times 10^6$, Ma = 0.85, $C_L = 0.5$)

Quantity	Baseline	Kriging optimization	GEK optimization
Drag coefficient C_D	0.02928	0.02808 (-4.1%)	0.02393 (-18.3%)
Total wing Mass, Kg	2374.58	2663.23 (+12.2%)	2295.43 (-3.3%)
Lift coefficient C_L	0.5	0.5	0.5
Moment coefficient C_M	-0.0917	-0.0826	-0.0917
Stress K-S	0.698	0.590	0.586

5. Conclusion

In this paper, an efficient aerostructural design optimization method combining coupled adjoint method with GEK model was developed. And the method is compared with the traditional Kriging method in aerostructural design optimizations of a 36-dimensional DPW-W1 wing and a 72-dimensional NASA CRM wing.

- 1) A coupled adjoint gradient analysis code is developed and verified against the DPW-W1 case. Results show that the gradients computed by the coupled adjoint method agree well with those of the finite-difference method, with a relative error of less than 5%. This indicates that the developed coupled adjoint code has high precision.
- 2) The efficiency of optimization is significantly improved by incorporating gradient information. In the high-dimensional analytical function test case, the GEK method does not require additional computational cost to achieve optimal solutions as dimensionality increases, indicating its promise for high-dimensional optimization problems.
- 3) The developed GEK model with coupled adjoint method achieves significantly better results compared to the traditional Kriging method. In the 36-dimensional DPW-W1 design optimization, the developed method reduces drag by 4 counts (-2.3%) and mass by 310 kg (-18.7%). In the 72-dimensional CRM wing case, the reductions are 53 counts (-18.3%) for drag and 79 kg (-3.3%) for mass. Moreover, the total computational cost required by the developed method is about 1/2 that of the traditional Kriging method.

6. Acknowledgments

This work was supported by the National Key Research and Development Program of China under Grant No. 2023YFB3002800 and the Youth Innovation Team of Shaanxi Universities.

7. Contact Author Email Address

Zhong-Hua Han, professor, hanzh@nwpu.edu.cn, corresponding author.

8. Copyright Statement

The authors confirm that they, and/or their company or organization, hold copyright on all of the original material included in this paper. The authors also confirm that they have obtained permission, from the copyright holder of any third party material included in this paper, to publish it as part of their paper. The authors confirm that they give permission, or have obtained permission from the copyright holder of this paper, for the publication and distribution of this paper as part of the ICAS proceedings or as individual off-prints from the proceedings.

References

- [1] Greitzer, E. M., Bonnefoy, P. A., DelaRosaBlanco E., et al., "N+3 Aircraft Concept Designs and Trade Studies", W.K. Lord: 2010.
- [2] Krein, A., Williams, G., "Flightpath 2050: Europe's Vision for Aeronautics", European Commission, Belgium, 2011.
- [3] Chen, H., "Multidisciplinary Design Optimization", In: Encyclopedia of Ocean Engineering. Springer, Singapore, 2021.
- [4] Adler, E. J. and Martins, J. R. A., "Efficient Aerostructural Wing Optimization Considering Mission Analysis", *Journal of Aircraft*, Vol. 27, No. 5, 2023, pp. 594-980.
- [5] Haftka, R. T., "Optimization of Flexible Wing Structures Subject to Strength and Induced Drag Constraints", *AIAA Journal*, Vol. 15, No. 8, 1977, pp. 1101–1106.
- [6] Maute, K., Nikbay, M., and Farhat, C., "Coupled Analytical Sensitivity Analysis and Optimization of Three-Dimensional Nonlinear Aeroelastic Systems", *AIAA Journal*, Vol. 39, No. 11, 2001, pp. 2051–2061.
- [7] Martins, J. R. A., Alonso, J. J., and Reuther, J. J., "Aero-Structural Wing Design Optimization Using High-Fidelity Sensitivity Analysis", *Proceedings of the CEAS Conference on Multidisciplinary Aircraft Design and Optimization*, Cologne, Germany, 2001.
- [8] Kenway, G. K. W., Kennedy, G. J., and Martins, J. R. R. A., "Aerostructural Optimization of the Common Research Model Configuration," 15th AIAA/ISSMO Multidisciplinary Analysisand Optimization Conference, Atlanta, GA, 2014.
- [9] Simpson, T.W., Booker, A. J., Ghosh, D., Giunta, A. A., Koch, P. N., and Yang, R.-J., "Approximation Methods in Multidisciplinary Analysis and Optimization: A Panel Discussion," *Structural and Multidisciplinary Optimization*, Vol. 27, No. 5, 2004, pp. 302–313.
- [10] Viana, F. A. C., Simpson, T. W., Balabanov, V., and Toropov, V., "Metamodeling in Multidisciplinary Design Optimization: How Far Have We Really Come?" *AIAA Journal*, Vol. 52, No.4, 2014, pp. 670–690.
- [11]Liu, J., Song, W.-P., Han, Z. H., and Zhang, Y., "Efficient Aerodynamic Shape Optimization of Transonic Wings Using a Parallel Infilling Strategy and Surrogate Models," *Structural and Multidisciplinary Optimization*, Vol. 55, No. 3, 2016, pp. 925–943.
- [12]Han, Z. H., "Improving Adjoint-Based Aerodynamic Optimization via Gradient-Enhanced Kriging," *50th AIAA Aerospace Sciences Meeting*, Nashville, Tennessee, 2012.
- [13]Han, Z. H., Zhang, Y., Song, C. X., and Zhang, K. S., "Weighted Gradient-Enhanced Kriging for High-Dimensional Surrogate Modeling and Design Optimization," *AIAA Journal*, Vol. 55, No. 12, 2017, pp. 4330–4346.
- [14]Laurenceau, J., Meaux, M., Montagnac, M., and Sagaut, P., "Comparison of Gradient-Based and Gradient-Enhanced Response-Surface-Based Optimizers," *AIAA Journal*, Vol. 48, No. 5, 2012, pp. 981–994.
- [15]Yamazaki, W., and Mavriplis, D. J., "Derivative-Enhanced Variable Fidelity Surrogate Modeling for Aerodynamic Functions," *AIAA Journal*, Vol. 51, No. 1, 2013, pp. 126–137.
- [16]Han, S. Q., Song, W. P., Han, Z. H., Wang, L., "Aerodynamic Inverse Design Method Based on Gradient-Enhanced Kriging Model", *Acta Aeronauticaet Astronautica Sinica*, Vol. 38, No. 7, 2017, pp. 120817-120817.
- [17]Mader, C. A., Kenway, G. K. W., Yildirim, A., and Martins, J. R. R. A., "ADflow—An Open-Source Compu- Tational Fluid Dynamics Solver for Aerodynamic and Multidisciplinary Optimization", *Journal of Aerospace Information Systems*, Vol. 17, No. 9, 2020, pp. 481-553.
- [18]Kenway, G. K. W., Mader, C. A., He, P. and Martins, J. R. A., "Effective Adjoint Approaches for Computational Fluid Dynamics", *Progress in Aerospace Sciences*, Vol. 110, 2019, p. 100542.
- [19]Boopathy, K., and Kennedy, G. J., "Parallel Finite Element Framework for Rotorcraft Multibody Dynamics and Discrete Adjoint Sensitivities", *AIAA Journal*, Vol. 57, No. 8, 2019, pp. 3111-3645.
- [20]Brown, S. A., "Displacement Extrapolation for CFD+CSM Aeroelastic Analysis," *Proceedings of the 38th AIAA Aerospace Sciences Meeting*, Kissimmee, Florida, 1997, AIAA 1997-1090.